

The Whole Is Greater than the Sum of Its Parts: Improving DNN-based Music Source Separation

Ryosuke Sawata, *Member, IEEE*, Naoya Takahashi, *Member, IEEE*, Stefan Uhlich, *Member, IEEE*, Shusuke Takahashi, *Member, IEEE*, and Yuki Mitsufuji, *Member, IEEE*,

Abstract—This paper presents the crossing scheme (X-scheme) for improving the performance of *deep neural network* (DNN)-based music source separation (MSS) without increasing calculation cost. It consists of three components: (i) *multi-domain loss* (MDL), (ii) *bridging operation*, which couples the individual instrument networks, and (iii) *combination loss* (CL). MDL enables the taking advantage of the frequency- and time-domain representations of audio signals. We modify the target network, i.e., the network architecture of the original DNN-based MSS, by adding bridging paths for each output instrument to share their information. MDL is then applied to the combinations of the output sources as well as each independent source, hence we called it CL. MDL and CL can easily be applied to many DNN-based separation methods as they are merely loss functions that are only used during training and do not affect the inference step. Bridging operation does not increase the number of learnable parameters in the network. Experimental results showed that the validity of Open-Unmix (UMX) and densely connected dilated DenseNet (D3Net) extended with our X-scheme, respectively called X-UMX and X-D3Net, by comparing them with their original versions. We also verified the effectiveness of X-scheme in a large-scale data regime, showing its generality with respect to data size. X-UMX Large (X-UMXL), which was trained on large-scale internal data and used in our experiments, is newly available at <https://github.com/asteroid-team/asteroid/tree/master/egs/musdb18/X-UMX>.

Index Terms—Music source separation (MSS), Deep neural network (DNN), Loss function

I. INTRODUCTION

THERE is a huge amount of music in our lives, e.g., from radio and TV, as background music in stores or provided by online streaming services. To specialize music for diverse purposes, it is sometimes necessary to remix it, e.g., making the vocal tracks louder, suppressing undesired instruments, or upmixing to more audio channels. It is easy for us to implement such operations when we have access to each audio source independently that was used to mix the music. However, if we only have access to the final recording, which is often the case, this is much more challenging. In such cases, it is necessary to separate music into each instrument, which is called music source separation (MSS), to achieve the above operations.

MSS has a long history and it is known to be a very challenging problem [2]; therefore, many approaches have

been investigated, e.g., local Gaussian modelling [3, 4], non-negative matrix factorization [5–7], kernel additive modelling [8], and combinations of these approaches [9, 10]. Data-driven machine learning approaches for MSS have also been of great interest to researchers. Many methods that use *deep neural networks* (DNNs) have been investigated to improve MSS performance. Specifically, introducing *multi-layer perceptrons* (MLPs) [11], *convolutional neural networks* (CNNs) [12], and *recurrent neural networks* (RNNs) [13], which are the three basic DNN architectures, have been used for MSS. An MLP was used to separate the input spectra then obtain separated results [14, 15]. CNNs and RNNs were used to achieve source separation with better quality [16–18] than previous MLP-based methods since the convolutional and recurrent layers of CNNs and RNNs can effectively capture the temporal contexts.

Although the above studies drastically improved MSS performance, there are two problems with respect to the training of music separation networks:

- (P1) Most DNN-based MSS methods tend to handle only the time- or frequency-domain but not both.
- (P2) They do not handle the mutual effect among output sources since network architectures and loss functions are independently computed for each estimated source and the corresponding ground-truth.

For example, a well-known open-source MSS method, called *Open-Unmix* (UMX) [19]¹, executes MSS only in the frequency-domain. It also applies the conventional *mean squared error* (MSE) loss function to individual pairs of estimated and corresponding ground-truth magnitude spectrograms for each instrument. In other words, UMX trains networks individually for each instrument, and achieves MSS by using all of each independent network one-by-one. In the field of speech enhancement (SE), which can be regarded as a case of audio source separation, there are methods for solving the above problems. For solving (P1), Kim *et al.* [20] showed the effectiveness of multi-domain processing via hybrid denoising networks, and Su *et al.* [21] reported that building two discriminators responsible for the time- and frequency-domains can enable effective denoising and dereverberation in their scheme of using *generative adversarial networks* (GANs). For solving (P2), from the classical SE methods such as Wiener filter [22], to current SE methods, e.g., noise-aware training [23] and noise-aware variational autoencoder [24], there are many situations in which knowing and using the information of the added noise is generally beneficial for the

Ryosuke Sawata, Naoya Takahashi, Shusuke Takahashi and Yuki Mitsufuji are with the Tokyo Laboratory, R&D Center, Sony Group Corporation, Japan. Stefan Uhlich is with the Sony Europe B.V., Stuttgart, Germany. This paper is an extended version of [1].

¹[https://github.com/sigsep/open-unmix-\[nnabla\]pytorch](https://github.com/sigsep/open-unmix-[nnabla]pytorch)

following extraction of the target speech. In MSS, other non-target sources can be similarly regarded as “noise”, and its information may be beneficial for the following target source separation. There is also research on using it for MSS using a Wiener filter [25], but it is used only as post-processing; thus, the information of other non-target sources is not used to train a DNN.

Inspired by these discussions, we first append an additional differentiable *short-time Fourier transform* (STFT) or *inverse STFT* (ISTFT) layer² during training only. Therefore, the application of both loss functions in the time as well as frequency domains, i.e., applying *multi-domain loss* (MDL), becomes feasible. To consider the relationship among output sources, we then bridge each instrument network by adding averaging operations if the original source separation is achieved by applying each independent instrument network to the input mixture. This is called bridging operation. For the bridged network to better determine the relationship among output instruments, we produce output spectrograms for instrument combinations and apply MDL to them. We call this loss computation combination loss (CL). The combination of bridging operation and CL helps the separation network determine the cause of an estimation error, i.e., which sources are leaking to the target instrument.

In summary, MDL solves (P1) since the separation network can help determine the estimation error in both time and frequency domains. Bridging operation and CL solve (P2) since they enable the separation network to handle the mutual relationships among the separated sources. We collectively call this “X-scheme”, which crosses the information among all sources with MDL. It is important to note that X-scheme can improve the performance of DNN-based MSS systems while maintaining the original calculation cost. This is because MDL and CL only affect the training step, thus do not change the original inference step. Moreover, bridging operation requires only a slight network modification but does not increase the number of parameters that need to be learned.

Although we confirmed the validity of X-scheme in our previously proposed DNN-based MSS method, i.e., extended UMX (X-UMX) [1] by applying X-scheme to UMX, there remains three questions: (i) its generality to other types of network architectures, (ii) the effective positions where we should bridge the paths of the target networks, and (iii) its scalability to a large-scale data regime. Hence, in this paper we address these questions. Specifically, we validate the effectiveness of X-scheme by applying it to different types of DNN-based MSS methods: well-known CNN-based and RNN-based ones, i.e., *densely connected dilated DenseNet* (D3Net) [26, 27] and *Open-Unmix* (UMX) [19]. We also present a detailed study regarding the bridging positions and potential to use a large dataset for training X-UMX.

The rest of this paper is organized as follows. In Section II, we give a brief review of related work. In Section III, we present X-scheme. In Section IV, we show the effectiveness of X-scheme by applying it to UMX and D3Net resulting in

X-UMX and X-D3Net in terms of the MSS task. Finally, we conclude this paper in Section V.

II. RELATED WORK

DNN-based MSS methods have been roughly categorized into time- and frequency-domain methods. UMX [19] receives the input spectrogram of a mixture song and extracts the target instrument by using fully connected and bi-directional long short-term memory (BLSTM) layers on the spectrogram, i.e., it works in the frequency domain. Similarly, D3Net [26, 27] extracts the target instrument from the input spectrogram by using convolutional layers in the frequency-domain. Note that they use a *multichannel Wiener filter* (MWF) [25] to reduce artifacts caused by non-linear separation due to DNN-based processing. Frequency-domain-based methods are powerful; thus, both methods recorded good scores on MUSDB18, which is a public dataset prepared for signal separation evaluation campaign (SiSEC) 2018 [28].

Time-domain methods directly operate on time-domain signals. To the best of our knowledge, Lluís *et al.* and Stoller *et al.* almost simultaneously started to explore time-domain MSS methods [29, 30]. However, the MSS performances of such methods are inferior to those of frequency-domain based methods. Specifically, the overall *signal-to-distortion ratio* (SDR) was reported to be only around 3.2 dB, which was almost 2 dB behind that of frequency-domain methods. Note that the experiments in the above studies were conducted on the same public dataset, i.e., MUSDB18; thus, we can compare their results. Défossez *et al.* then investigated a new time-domain method, Demucs [31], which is based on Wave-U-net [30]. Demucus improves the modelling capability by incorporating gated linear unit layers [32], BLSTM, and faster strided convolutions, thus it demonstrated competitive results to frequency-domain methods on MUSDB18.

Although both time- and frequency-domain methods have recorded good MSS performance, there are still concerns. Almost all DNN-based frequency-domain methods tend to use only a spectrogram without phase information since it is difficult for DNNs to receive imaginary variables. The phase information is often ignored with such methods. Therefore, the phase of the input mixture is often used with the output magnitude spectrogram to apply ISTFT, although it must not match the target source’s spectrogram. The Fourier basis, which is used to calculate the above spectrogram, is not always optimal for DNN-based MSS methods. Time-domain methods, however, can optimize their networks from the perspective of being end-to-end, i.e., including the phase information, but tend to make the training difficult. Inspired by this insight, we previously proposed X-UMX, which can use time-domain information via MDL [1], and confirmed it performed better than UMX. Methods using time and frequency information in a hybrid manner were proposed for DNN-based MSS. For example, KUIELAB-MDX-Net [33] and Danna-Sep [34] are hybrid methods using time and frequency features. Specifically, they combine the heterogeneous time- and frequency-based MSS networks on the basis of the blending scheme [35], resulting in high performing hybrid MSS.

²If the network outputs a spectrogram, we append an ISTFT layer whereas an STFT layer is added if the network output is a time signal.

The number of methods using complex-valued features, i.e., spectrogram magnitude and the corresponding phase via STFT, for MSS has been increasing [36–38]. Specifically, *latent source attentive frequency transformation* (LaSAFT) [36] and its light version, LightSAFT [37], use *complex-as-channels* (CaC) [39] built on U-net [40], enabling MSS in the complex-valued domain. Défossez *et al.* also improved upon the original Demucs by using CaC, called Hybrid Demucs [41], to use time as well as complex-valued frequency information. It has two branches in the network architecture and each handles time or complex-valued frequency input. Liu *et al.* proposed *channel-wise subband phase-aware ResUNet* (CWS-PRResUNet) [38] which includes phase estimation by using the loss function of *complex ideal ratio mask* (cIRM) [42]. Their motivations, which involve phase information as well as spectrogram magnitude, are similar to those of the hybrid methods that compensate for the missing phase information by adding the time-domain signal. Therefore, the above complex-domain methods are related to hybrid methods.

There have been several attempts to directly estimate the phase of the target source [43, 44]. PhaseNet [43] successfully predicts the phase information by defining the phase-estimation problem as a classification of discretized phase values. DiffPhase [45] generates as well as predicts the phase through the framework of a diffusion-based generative model, which it is suitable for the given spectrogram magnitude. The authors reported that the perceptual scores of reconstructed time signals were high even when their phases were partially generated.

From this literature review, we can see that using the time domain or similar features as well as the frequency domain is important to achieve good MSS performance. However, changing the network architecture such that the time- and frequency-domain features input are acceptable and optimizing this new architecture may be a laborious task. X-scheme, which includes MDL, is very simple and easy to use, thus enables many methods to handle both the time- as well as frequency-domain features in a hybrid manner.

III. X-SCHEME FOR DNN-BASED MSS

In this section, we describe X-scheme, which consists of three components, i.e., MDL, bridging operation, and CL. As mentioned in Sec. I, MDL should solve (P1) and bridging operation and CL should solve (P2).

Throughout the paper, we use the following notations. We first assume that the time-domain mixture signal \mathbf{x} consists of J sources, i.e.,

$$\mathbf{x} = \sum_{j=1}^J \mathbf{y}_j, \quad (1)$$

where \mathbf{y}_j denotes the time-domain signal of the j th source. Note that \mathbf{x} and \mathbf{y}_j are column vectors with their samples. The DNN then predicts the spectrogram of the j th target source from the input mixture spectrogram $\mathbf{X} = \mathcal{S}\{\mathbf{x}\}$:

$$\hat{\mathbf{y}}_j = \mathcal{S}^{-1}\{\hat{\mathbf{Y}}_j\}, \quad (2)$$

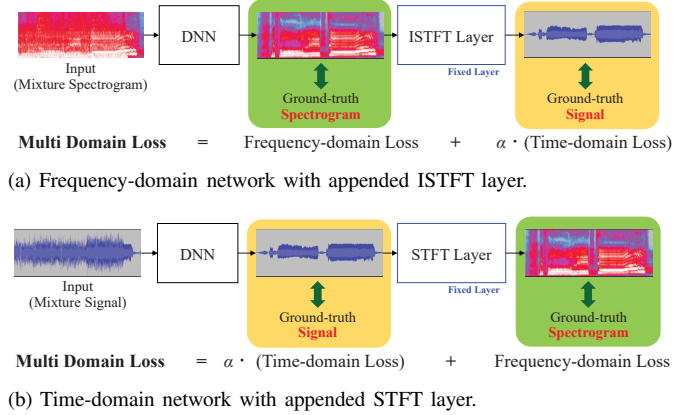


Fig. 1. MDL. Note that α is scaling parameter.

where \mathcal{S} and \mathcal{S}^{-1} represent the operators of STFT and inverse STFT (ISTFT), respectively. A variable with the hat symbol, e.g., $\hat{\bullet}$, denotes the results estimated with the DNN. Therefore, $\hat{\mathbf{y}}_j$ and $\hat{\mathbf{Y}}_j$ are respectively the predicted time- and frequency-domain results of ground truths, i.e., \mathbf{y}_j and \mathbf{Y}_j , via the DNN.

A. Multi-domain Loss

For MDL, we first append an additional differentiable and fixed STFT or ISTFT layer after the final layer of the target DNN, as shown in Fig. 1. It is then possible to calculate the loss functions in both time- and frequency-domains before and after the appended layer. Since this appended layer is only used during training for computing MDL, it does not affect the inference step. In X-scheme, we use the loss functions of the MSE and *weighted signal-to-distortion ratio* (wSDR) [46] as the frequency- and time-domains, i.e.,

$$\mathcal{L}_{\text{MDL}}^J = \mathcal{L}_{\text{MSE}}^J + \alpha \left(\mathcal{L}_{\text{wSDR}}^J + 1.0 \right), \quad (3)$$

where α is a scaling parameter for mixing multiple domains of loss. Specifically, $\mathcal{L}_{\text{MSE}}^J$ and $\mathcal{L}_{\text{wSDR}}^J$ are respectively calculated as follows:

$$\mathcal{L}_{\text{MSE}}^J = \sum_{j=1}^J \sum_{t,f} \left\{ |Y_j(t, f)| - |\hat{Y}_j(t, f)| \right\}^2, \quad (4a)$$

$$\mathcal{L}_{\text{wSDR}}^J = \sum_{j=1}^J \left\{ -\rho_j \frac{\mathbf{y}_j^T \hat{\mathbf{y}}_j}{\|\mathbf{y}_j\| \|\hat{\mathbf{y}}_j\|} - (1 - \rho_j) \frac{(\mathbf{x} - \mathbf{y}_j)^T (\mathbf{x} - \hat{\mathbf{y}}_j)}{\|\mathbf{x} - \mathbf{y}_j\| \|\mathbf{x} - \hat{\mathbf{y}}_j\|} \right\}, \quad (4b)$$

where t and f denote the indexes of the time frame and frequency bin of the spectrogram $Y_j(t, f)$, respectively. In addition, ρ_j is the energy ratio between the j th source \mathbf{y}_j and mixture \mathbf{x} in the time-domain, i.e., $\rho_j = \|\mathbf{y}_j\|^2 / (\|\mathbf{y}_j\|^2 + \|\mathbf{x} - \mathbf{y}_j\|^2)$. Note that the output range of the wSDR in Eq. (4b) is bounded to $[-1, 1]$. Therefore, $(\mathcal{L}_{\text{wSDR}}^J + 1.0)$ written in Eq. (3) is bounded to $[0, 2.0]$, and it is useful to mix with another type of loss, i.e., MSE in our case. Although the SDR is traditionally calculated including the logarithm, we keep the no-logarithm style and use Eq. (4b) for MDL due to the above reason.

By using MDL, the target DNN can leverage the advantage of both domains even if the original network operates in

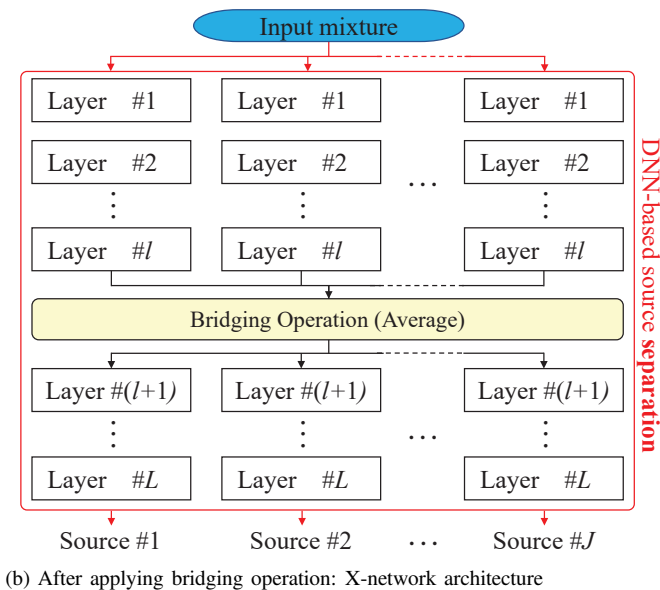
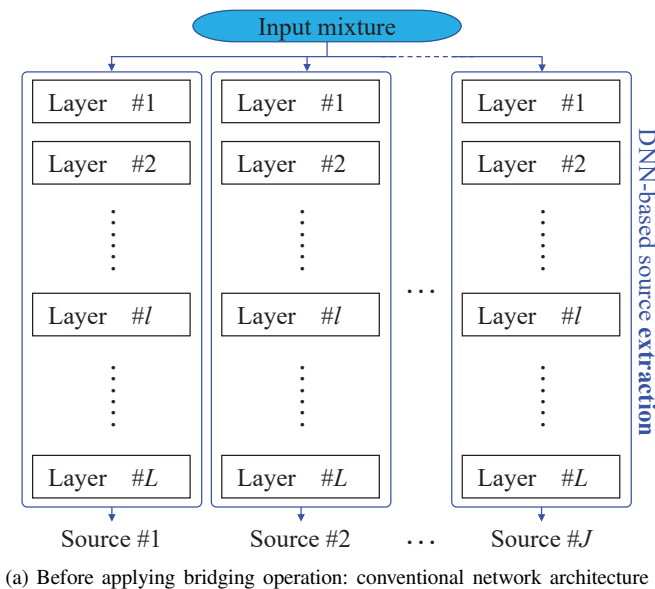


Fig. 2. Comparison of applying and not applying bridging operation

either one of them. MDL can also be applied to many conventional DNN-based MSS methods by simply replacing the loss function; thus, no additional calculation is required during the inference.

B. Combination Schemes

In this subsection, we explain bridging operation for DNN-based MSS (Sec. III-B1) and CL (Sec. III-B2) to help independent extraction networks support each other.

1) *Bridging Operation*: As shown in the blue rectangle of Fig. 2(a), if DNN-based MSS is achieved using independent instrument networks, it is difficult for each network to take into account their mutual effect. Thus, we argue that it is effective to cross the network graphs to help independent sub-networks

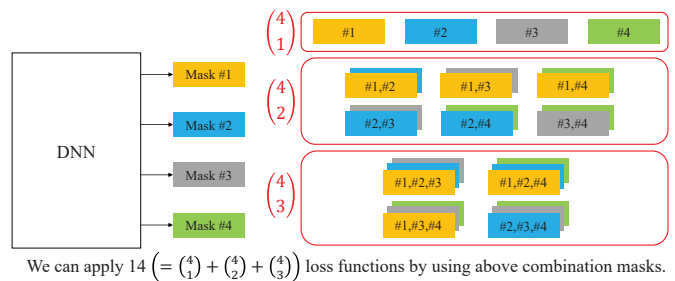


Fig. 3. CL when mixture consists of four sources

support each other³. This is the reason X-scheme includes bridging operation. However, we previously did not investigate the detailed settings of bridging operation such as its position and numbers. As shown in Fig. 2(b), it is possible to place a bridge between layers l and $(l+1)$. We can place multiple bridges depending on the number of target network layers L , namely, we can place up to $(L-1)$ bridges. Namely, we connect the paths to cross each source's networks by adding one or more average operators to the original network. Note that bridging operation does not have any learnable parameters; thus, the calculation cost slightly increases compared with the original network due to merely adding a few averaging operations. We can then regard the parts before and after the last added bridge as the interaction and each source extraction part; thus, their capacity depending on the position of bridging affects the final MSS performance. Motivated by the above discussion, we will conduct experiments on X-UMX (Sec. IV-A) to confirm the effect of the number and position of bridging operation on MSS performance.

2) *Combination Loss*: As mentioned above, the purpose of applying bridging operation is to enable each source-extraction network to handle the relationship among output sources via built bridges. In other words, it is necessary for each source-extraction network to learn its mutual relationships during training. However, using only bridging operation is insufficient for the networks to work together if the loss function is computed independently for each instrument. Thus, it is effective to cross the loss function as well as network paths via CL to boost the benefit of the built bridges. For CL, we consider the combinations of output spectrograms to enable each DNN-based source extractor to interact with each other. Specifically, we combine two or more estimated spectrograms into new ones, where each one can extract two or more sources from the mixture. Using the newly obtained combination spectrograms enables us to compute more loss functions than when we use only the individual instrument spectrograms independently, i.e.,

$$\mathcal{L} = \frac{1}{N} \sum_{n=1}^N \mathcal{L}_{\text{MDL}}^n, \quad (5)$$

³Note that bridging operation may be only needed for methods such as UMX, since it consists of individual extraction networks. In other words, this bridging is not necessary for methods that learn one network for all sources such as Demucs [31].

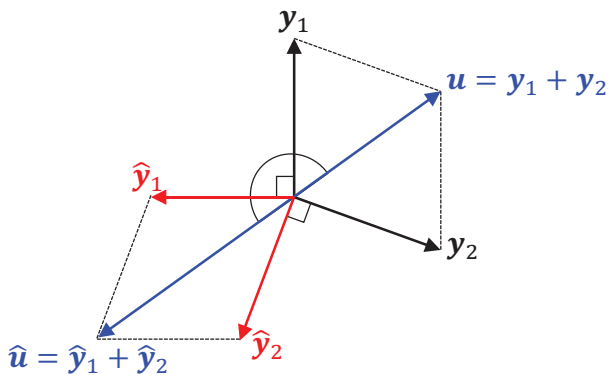


Fig. 4. Example of angles consisting of ground-truth signals (y_1, y_2, u) and their corresponding predicted ($\hat{y}_1, \hat{y}_2, \hat{u}$). Black and red arrows denote ground truth and corresponding predicted signals, respectively. Blue arrows denote combined signals.

where $N > J$ is the total number of possible combinations except for mixing all J sources, i.e., $N = \sum_{i=1}^{J-1} \binom{J}{i}$, and n denotes the index of the n th combination⁴. For instance, when separating $J = 4$ sources, as is the case with MUSDB18, we can consider 14 ($= \sum_{i=1}^{4-1} \binom{4}{i}$) combinations in total, as shown in Fig. 3, whereas conventional methods handle only each source independently, i.e., 4 source spectrograms.

To explain the advantage of CL, let us consider the following example. Assume that we have a system with leakage of *vocals* into *drums* and *bass* resulting in similar errors that both instruments exhibit. By considering the combination *drums* + *bass*, we notice that the two errors are correlated, resulting in an even larger leakage of vocals, which we try to mitigate using CL. More formally, let ϵ_j denote the prediction error of the j th source; $\hat{y}_j = y_j + \epsilon_j$. We can then consider the MSE of the combination $u = y_1 + y_2$:

$$\begin{aligned} \text{MSE}(u, \hat{u}) &= \text{E}[(u - \hat{u})^2] \\ &= \text{E}[\{(y_1 + y_2) - (y_1 + \epsilon_1 + y_2 + \epsilon_2)\}^2] \\ &= \text{E}[\epsilon_1^2 + 2\epsilon_1\epsilon_2 + \epsilon_2^2]. \end{aligned}$$

When we consider y_1 and y_2 separately without the combination, the term “ $2\epsilon_1\epsilon_2$ ” does not appear in the MSE; $\text{MSE}(y_1, \hat{y}_1) + \text{MSE}(y_2, \hat{y}_2) = \text{E}[\epsilon_1^2 + \epsilon_2^2]$. Therefore, by using CL, we can monitor the error correlation term “ $\text{E}[2\epsilon_1\epsilon_2]$ ”, which helps the source-extraction networks train when they are correlated. We can also analyze CL in terms of a geometrical viewpoint. Focusing on Eq. (4b), since the wSDR consists of two cosine similarity functions, it monitors the angle consisting of the ground truth y_j and corresponding predicted \hat{y}_j . However, there is a critical case in which the prediction error cannot be detected in terms of the cosine similarity. As shown in Fig. 4, when the predicted \hat{y}_1 and \hat{y}_2 are respectively orthogonal to the corresponding ground truth y_1 and y_2 , it is difficult to detect the prediction error since $\cos(y_1, \hat{y}_1)$ and $\cos(y_2, \hat{y}_2)$ are both zeros. However, CL can detect its prediction error via the combined signals u and \hat{u}

⁴Initial experiments showed that the combination ${}_J C_J$, i.e., adding and mixing all sources, does not further improve MSS performance, thus it is not used in Eq. (5).

since the score of $\cos(u, \hat{u}) = -1$ penalizes the target network by substituting it for the wSDR-based loss function.

Independent sub-networks can detect each other via the added bridges and CL. The DNN-based MSS network extended with X-scheme can handle multiple sources together, i.e., separate two or more sources, rather than each source independently. From a different viewpoint, CL can be considered to provide a similar benefit to multi-task learning [47] since it handles multiple objectives jointly by computing combinational loss functions.

We can apply X-scheme to many DNN-based MSS methods to improve their performances while maintaining almost the same computational cost as the original method since MDL and CL are merely loss functions and bridging operation is achieved with simple average operations without increasing learnable parameters. As discussed in Sec. IV, X-scheme improves DNN-based MSS performance.

IV. EXPERIMENTS

In this section, we present our experiments on X-scheme for MSS. We first explore the effect of the bridging position using X-UMX [1] to provide insights on the optimal position and its sensitivity. Next, we confirm the scalability of X-scheme in a large-scale data regime. Finally, we demonstrate the generality of X-scheme by applying it to another type of network architecture, D3Net.

We used the following datasets and STFT/ISTFT settings for the experiments:

MUSDB18 [48]

The MUSDB18 dataset is comprised of 150 songs, each of which was recorded at a 44.1-kHz sampling rate. It consists of two subsets (“train” and “test”), where we further split the train set into “train” and “valid” as defined in the official “musdb” package⁵. For each song, the mixture and its four sources, i.e., *bass*, *drums*, *other* and *vocals*, are available.

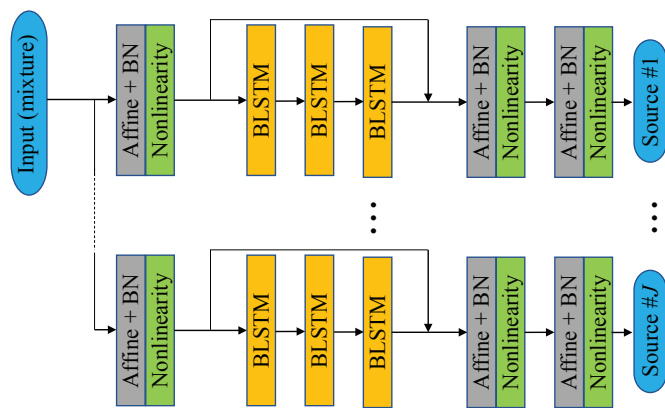
STFT/ISTFT

We used a Hann window with a length of 4096 samples and 75% overlap. We used STFT magnitudes obtained from the mixture signal as input and trained networks to estimate target mask $M_j(t, f)$ or spectrograms $Y_j(t, f)$, where f is the frequency bin and t the frame index.

A. X-UMX

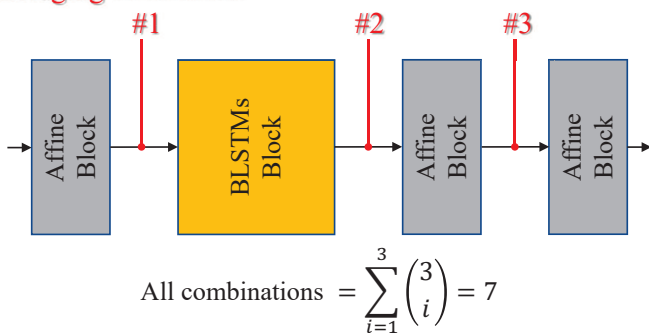
The network architecture of UMX is illustrated in Fig. 5(a). The network was trained to estimate all the sources’ masks with the Adam [49] optimizer for 1,000 epochs. The learning rate was set to 0.001 with a weight decay of 0.00001. The batch size was set to 14 and each input was a random crop of 6.0 sec from the dataset. The scaling parameter α , introduced in Eq. (3) for MDL, was set to 10.0 to approximately equalize

⁵<https://github.com/sigsep/sigsep-mus-db/blob/master/musdb/configs/mus.yaml>



(a) UMX

Bridging candidates:



(b) Candidates of bridging operation on UMX

Fig. 5. Original network architecture of UMX and its bridging candidates

the ranges of $\mathcal{L}_{\text{MSE}}^J$ and $\mathcal{L}_{\text{wSDR}}^J$ by looking at each loss function’s learning curves, respectively. Note that the details of other settings are shown in our code⁶ and previous paper [1].

1) *Bridging positions*: As shown in Fig. 2, bridging operation can be applied to arbitrary positions between the layers. The number of bridges can also be increased depending on the number of gaps between adjacent layers. Therefore, in this section, we present the results regarding the position of bridging operation on X-UMX trained under the same configurations, e.g., the number of epochs, regularization parameters, and type of optimizer, as mentioned in the previous subsection. We show the simplified network architecture and possible bridging candidates of UMX in Fig. 5(b). UMX roughly consists of three affine blocks and a BLSTM block. Each affine block has a fully connected layer, batch normalization layer, and activation function. The BLSTM block has three consecutive BLSTM layers with dropout. In this experiment, we considered three positions as candidates for inserting the bridging network and examined the performance for all combinations of bridging position.

The results are shown in Fig. 6. The performances of almost all bridged versions of UMX, i.e., bridging position (BP) from 1 to 7 (BP1-BP7), were superior to the baseline from the perspective of source-to-interference ratio (SIR) and source image-to-spatial distortion ratio (ISR) (see “Avg.” of Figs. 6(b)

⁶<https://github.com/asteroid-team/asteroid/tree/master/egs/musdb18/X-UMX>

TABLE I
COMPARISON OF X-UMX WITH UMX IN TERMS OF SDR
 (“MEDIAN OF FRAMES, MEDIAN OF TRACKS”).

Method	Dataset Size	Bass	Drums	Other	Vocals	Avg.
UMX [19]	10h (MUSDB18)	5.23	5.73	4.02	6.32	5.33
X-UMX		5.43	6.47	4.64	6.61	5.79
UMXL	100h (INTERNAL)	5.79	6.93	4.50	6.71	5.98
X-UMXL		6.28	7.39	4.83	7.57	6.52
Public UMXL [†]	500h	6.02	7.15	4.89	7.21	6.32

[†] <https://zenodo.org/record/5069601>

and (c)). Only the SIR result of BP1 did not outperform that of the baseline, but was comparable. Hence, we argue that bridging operation can improve the suppression of the other interference instruments without increasing linear distortions since ISR becomes low when the output signal increases linear distortions. Focusing on the sources-to-artifacts ratio (SAR) results, we can confirm that some versions were inferior to the baseline (see “Avg.” of Fig. 6(d)). Specifically, there were combinations with no-good SAR results, e.g., BP1 and BP7, since their scores were inferior to that of the baseline. The commonality of BP1 and BP7 is that at least one of their positions was too shallow or deep. From these results, we can assume that certain depths are required before and after bridging operation to improve the SAR. Focusing on the SDR results, which were computed by summing up the weighted SIR, ISR and SAR, we argue that X-UMX outperformed UMX because the SDR results of BP1-BP7 improved in most cases compared with that of the baseline (see Fig. 6(a)). In particular, BP4, which bridged the paths between “Affine Block” and “BLSTMs Block”, performed the best in terms of the SDR. Hence, bridging paths between the gaps of different type of blocks or layers is probably effective in terms of sharing each sub-extraction network’s information.

2) *Scalability with large training datasets*: In this section, we discuss the potential of X-UMX for a large-scale training dataset, i.e., X-UMXL, which was not assessed in our previous study [1]. DNNs can generalize well if enough data is available for training, and some regularization methods might become ineffective in such a case. Thus, it is important to investigate the scalability of X-scheme. Specifically, we trained UMX and X-UMX on an internal dataset consisting of 1505 songs with a total duration of approximately 100 h, which is 10 times larger than MUSDB18. We denote this dataset as “INTERNAL”. Each song of INTERNAL consists of four instruments, as in MUSDB18.

The results are summarized in Table I. X-UMX and X-UMXL outperformed the corresponding UMX and UMXL if they were trained on the same dataset, i.e., using MUSDB18 or INTERNAL. X-UMX and X-UMXL outperformed the original UMX and UMXL for all instruments (see the boldface in Table I). This shows that X-scheme is effective even when we have more training data available.

It is worth noting that X-UMXL greatly outperformed not only our self-implemented UMXL trained on INTERNAL but also “public UMXL”, which was provided by the authors of

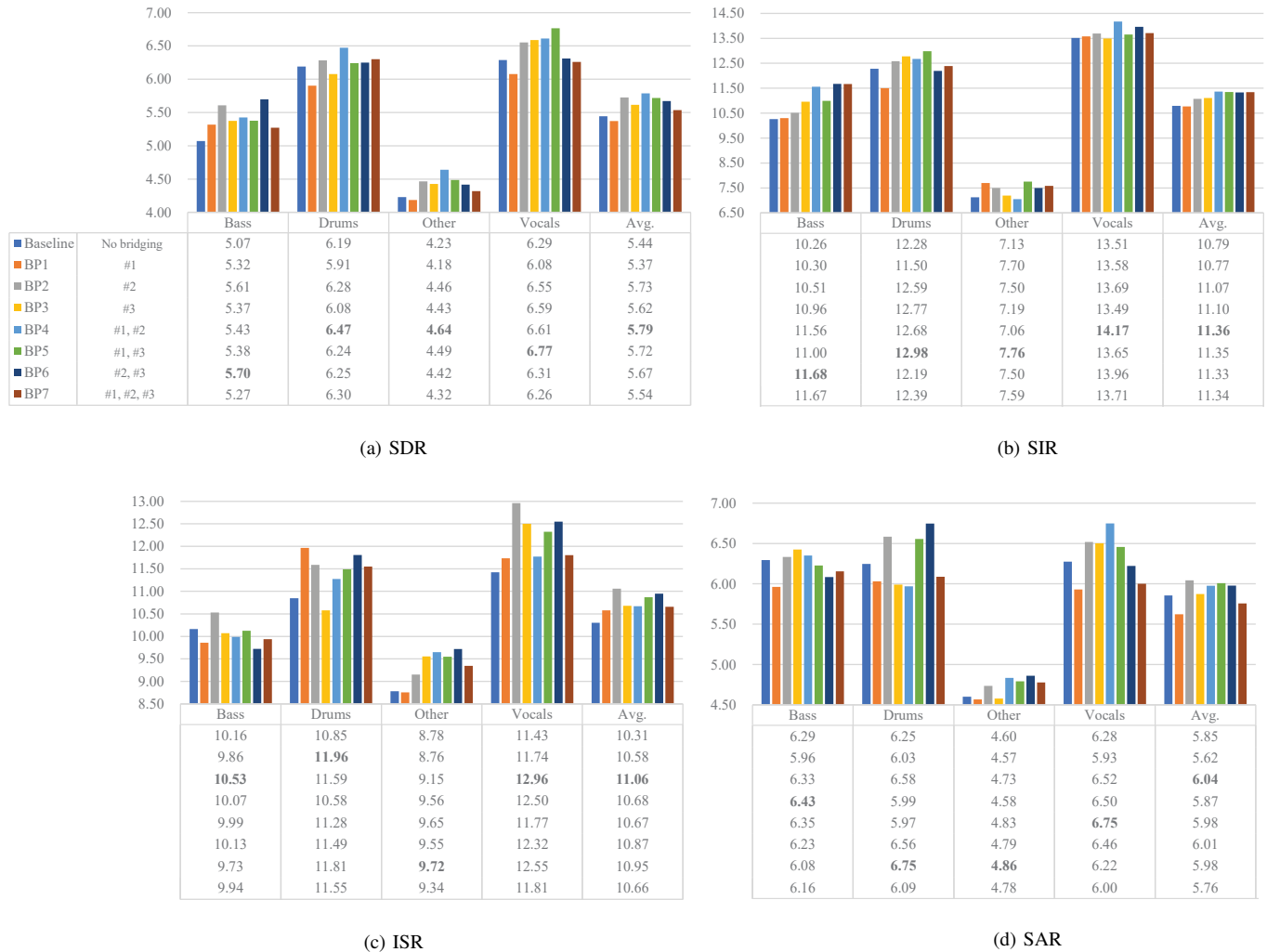


Fig. 6. Results regarding bridging position(s) for X-UMX. Note that correspondence between bridging indexes written in (a) and positions are shown in Fig. 5(b).

UMX, although the size of our dataset is one fifth of theirs⁷ (see the yellow highlighted cells in Table I). From these results, we argue that X-scheme can use a given dataset for training more successfully, and even outperform a traditional setup with more training data.

B. X-D3Net

Next, we integrated X-scheme into D3Net resulting in X-D3Net. The network architecture is shown in Fig. 7. The original D3Net, C1, uses band-wise MDenseNets [16] and integrated their outputs by applying a dense block, but they are independent of each other, i.e., there is no path to share their relationship among them. Hence, the bridging path is added at the end of band-wise D3 blocks, resulting in X-D3Net, as in the experiment in Sec. IV-A1. This suggests that the semantic boundary can be a good position for inserting bridging operation. The differences in network the architecture between D3Net and X-D3Net are shown in Fig. 7. Each network of X-D3Net was trained to estimate all the sources’

⁷The size of dataset used for training UMXL, i.e., 500 h, was confirmed with the developers.

spectrograms with the Adam [49] optimizer for 70 epochs. The initial learning rate was set to 0.001 with a weight decay of 0.00001, and its learning rate was dropped to 0.0003 and 0.0001 after 40 and 60 epochs, respectively. The batch size was set to 6 and each input was a randomly cropped music spectrogram with 352 frames. The scaling parameter α was set again to 10, as we did for X-UMX.

The results are shown in Fig. 8. Note that ‘P’ denotes the proposed method that includes all components of X-scheme, i.e., MDL, bridging operation, and CL, while ‘C1-C7’ denote the comparative methods lacking some of these components in order to confirm their effectiveness one-by-one. In terms of the SDR, the methods using at least one component of X-scheme, i.e., C2-C7 and P, were superior to D3Net, i.e., C1 (see the average performances denoted as ‘Avg.’ in Fig. 8(a)). Therefore, the validity of each component of X-scheme was confirmed on a CNN-based MSS method (D3Net) as well as an RNN-based MSS method (UMX). Overall, we could improve MSS performance by 0.3 dB.

In particular, the positive effect of MDL was notable compared with our previous corresponding results on X-UMX [1]

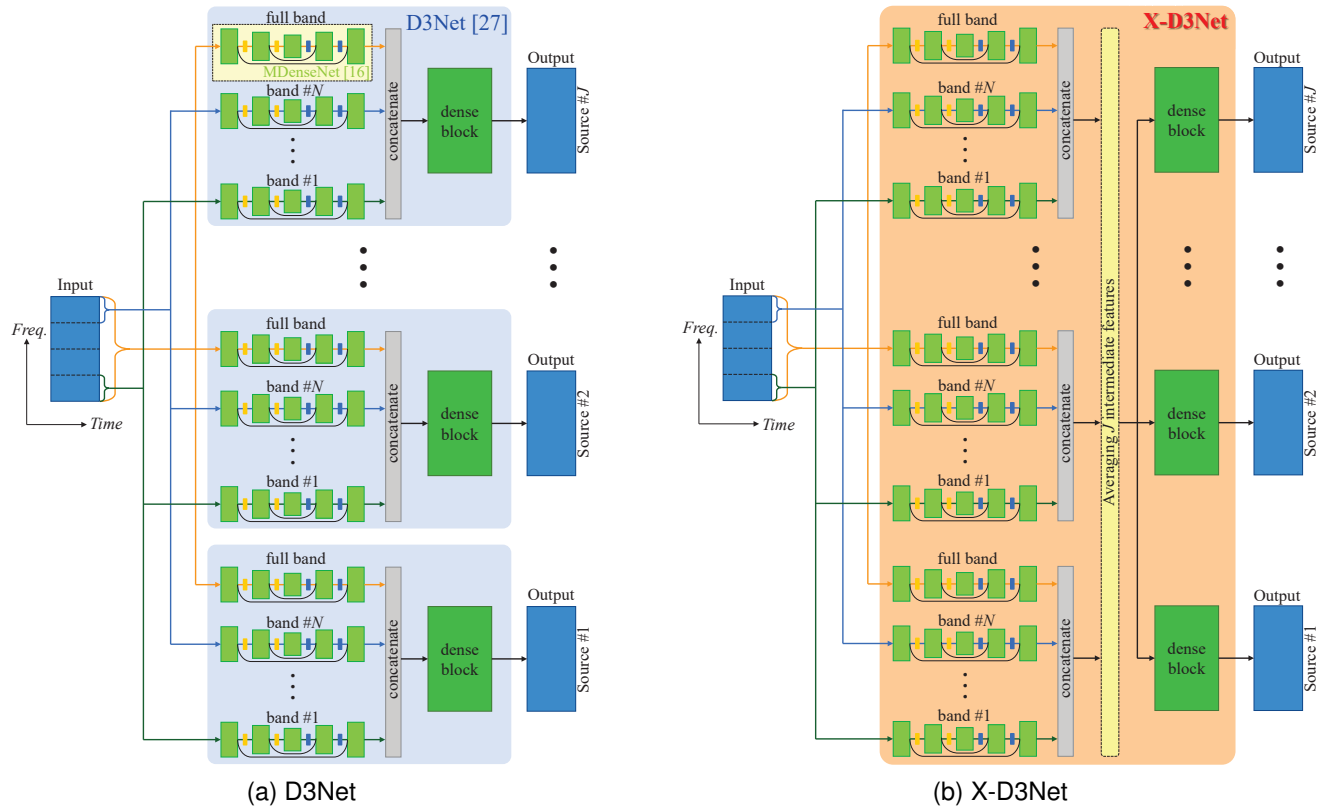


Fig. 7. Comparison of D3Net and X-D3Net

(see the results of methods including MDL, i.e., C2, C5, C6, and P). Therefore, regardless of whether the target network is an originally integrated one or tied against independent source sub-networks, the loss-function-related core components of X-scheme, i.e., MDL and CL, can improve MSS performance.

V. CONCLUSION

We revisited our previous proposal and summarized its core component, a versatile scheme called X-scheme. X-scheme consists of three parts: i) MDL, ii) bridging operation, and iii) CL, which improve the performance of DNN-based MSS with almost no increase in calculation cost. Specifically, as MDL and CL are merely loss functions used during training, they do not affect the computational cost at inference. As shown in Fig. 2, bridging operation does not increase calculation cost due to adding only a few average computations. To verify X-scheme for another type of network that differs from the recurrent type, i.e., UMX, we derived an X-scheme-based convolutional network in this paper. This MSS method is an extended version of D3Net, called X-D3Net. We confirmed its validity through experiments. We also examined the effectiveness of X-UMX through the following experiments: a) searching for the effective bridging position(s) and b) using a larger dataset than MUSDB18. X-UMXL, obtained by training X-UMX on our large-scale data regime (INTERNAL), greatly outperformed the public UMXL, although the size of our dataset is about 20% that of the private training dataset for public UMXL. Therefore, by sharing the information regarding the progress of MSS among all sub-networks, our X-scheme-based MSS method can versatilely improve MSS performance

more effectively than the original method. It is worth noting that X-scheme has high practicability since its components, i.e., MDL, CL, and bridging operation, have almost no effect on the inference of the original target method, and are easy to implement.

REFERENCES

- [1] R. Sawata, S. Uhlich, S. Takahashi, and Y. Mitsufuji, "All For One And One For All: Improving Music Separation By Bridging Networks," in *Proc. of IEEE International Conference on Acoustics, Speech and Signal Processing (ICASSP)*, 2021, pp. 51–55.
- [2] E. Cano, D. FitzGerald, A. Liutkus, M. D. Plumbley, and F.-R. Stöter, "Musical source separation: An introduction," *IEEE Signal Processing Magazine*, vol. 36, no. 1, pp. 31–40, 2019.
- [3] N. Q. K. Duong, E. Vincent, and R. Gribonval, "Under-determined reverberant audio source separation using a full-rank spatial covariance model," *IEEE Trans. on Audio, Speech, and Language Processing*, vol. 18, no. 7, pp. 1830–1840, 2010.
- [4] D. FitzGerald, A. Liutkus, and R. Badeau, "PROJET — Spatial audio separation using projections," in *Proc. of IEEE International Conference on Acoustics, Speech and Signal Processing (ICASSP)*, 2016, pp. 36–40.
- [5] A. Liutkus, D. Fitzgerald, and R. Badeau, "Cauchy nonnegative matrix factorization," in *Proc. of IEEE Workshop on Applications of Signal Processing to Audio and Acoustics (WASPAA)*, 2015, pp. 1–5.

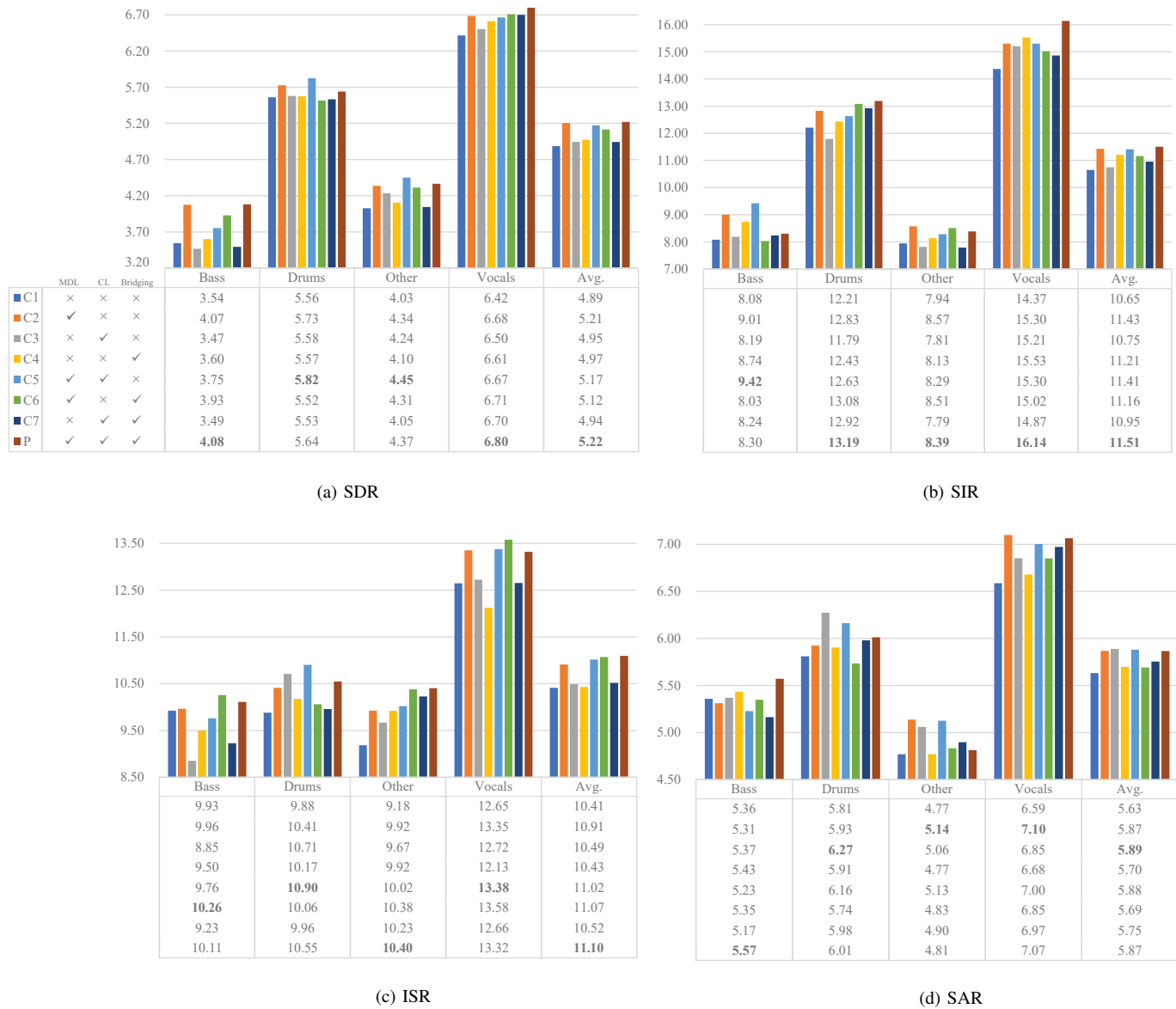


Fig. 8. Experimental results of X-D3Net. Note that conventional D3Net, which is denoted as “C1”, was re-trained for this experiment to equalize number of optimizers with X-D3Net’s. Namely, each version of X-D3Net was trained on single optimizer while original paper trained four D3Nets, each of which corresponds to each instrument, using four optimizers separately. Thus, results of C1 are different from those of original paper.

- [6] J. Le Roux, J. R. Hershey, and F. Weninger, “Deep nmf for speech separation,” in *Proc. of IEEE International Conference on Acoustics, Speech and Signal Processing (ICASSP)*, 2015, pp. 66–70.
- [7] Y. Mitsufuji, S. Koyama, and H. Saruwatari, “Multi-channel blind source separation based on non-negative tensor factorization in wavenumber domain,” in *Proc. of IEEE International Conference on Acoustics, Speech and Signal Processing (ICASSP)*, 2016, pp. 56–60.
- [8] A. Liutkus, D. Fitzgerald, Z. Rafii, B. Pardo, and L. Daudet, “Kernel additive models for source separation,” *IEEE Trans. on Signal Processing*, vol. 62, no. 16, pp. 4298–4310, 2014.
- [9] A. Ozerov and C. Fevotte, “Multichannel nonnegative matrix factorization in convolutive mixtures for audio source separation,” *IEEE Trans. on Audio, Speech, and Language Processing*, vol. 18, no. 3, pp. 550–563, 2010.
- [10] A. Liutkus, D. Fitzgerald, and Z. Rafii, “Scalable audio separation with light kernel additive modelling,” in *Proc. of IEEE International Conference on Acoustics, Speech and Signal Processing (ICASSP)*, 2015, pp. 76–80.
- [11] F. Rosenblatt, *Principles of Neurodynamics: Perceptrons and the Theory of Brain Mechanisms*, Defense Technical Information Center, 1961.
- [12] K. Fukushima, “Neocognitron: A self-organizing neural network model for a mechanism of pattern recognition unaffected by shift in position,” *Biological Cybernetics*, vol. 36, pp. 193–202, 1980.
- [13] D. E. Rumelhart, G. E. Hinton, and R. J. Williams, “Learning representations by back-propagating errors,” *Nature*, vol. 323, no. 6088, pp. 533–536, 1986.
- [14] A. A. Nugraha, A. Liutkus, and E. Vincent, “Multi-

- channel music separation with deep neural networks,” in *Proc. of 24th European Signal Processing Conference (EUSIPCO)*, 2016, pp. 1748–1752.
- [15] S. Uhlich, F. Giron, and Y. Mitsufuji, “Deep neural network based instrument extraction from music,” in *Proc. of IEEE International Conference on Acoustics, Speech and Signal Processing (ICASSP)*, 2015, pp. 2135–2139.
- [16] N. Takahashi and Y. Mitsufuji, “Multi-scale multi-band densenets for audio source separation,” in *Proc. of IEEE Workshop on Applications of Signal Processing to Audio and Acoustics (WASPAA)*, 2017, pp. 21–25.
- [17] S. Uhlich, M. Porcu, F. Giron, M. Enenkl, T. Kemp, N. Takahashi, and Y. Mitsufuji, “Improving music source separation based on deep neural networks through data augmentation and network blending,” in *Proc. of IEEE International Conference on Acoustics, Speech and Signal Processing (ICASSP)*, 2017, pp. 261–265.
- [18] N. Takahashi, N. Goswami, and Y. Mitsufuji, “MM-DenseLSTM: An efficient combination of convolutional and recurrent neural networks for audio source separation,” in *Proc. of IWAENC*, 2018.
- [19] F.-R. Stöter, S. Uhlich, A. Liutkus, and Y. Mitsufuji, “Open-Unmix - A reference implementation for music source separation,” *Journal of Open Source Software*, vol. 4, pp. 1667, 09 2019.
- [20] J.-H. Kim, J. Yoo, S. Chun, A. Kim, and J.-W. Ha, “Multi-domain processing via hybrid denoising networks for speech enhancement,” *arXiv*, 2018.
- [21] J. Su, Z. Jin, and A. Finkelstein, “HiFi-GAN: High-fidelity denoising and dereverberation based on speech deep features in adversarial networks,” in *Proc. of Interspeech*, 2020 (accepted for publication).
- [22] N. Wiener, *Extrapolation, Interpolation, and Smoothing of Stationary Time Series: With Engineering Applications*, The MIT Press, 08 1949.
- [23] J. Lee, Y. Jung, M. Jung, and H. Kim, “Dynamic noise embedding: Noise aware training and adaptation for speech enhancement,” in *Proc. of Asia-Pacific Signal and Information Processing Association Annual Summit and Conference (APSIPA ASC)*, 2020, pp. 739–746.
- [24] H. Fang, G. Carbajal, S. Wermter, and T. Gerkmann, “Variational autoencoder for speech enhancement with a noise-aware encoder,” in *Proc. of IEEE International Conference on Acoustics, Speech and Signal Processing (ICASSP)*, 2021, pp. 676–680.
- [25] A. A. Nugraha, A. Liutkus, and E. Vincent, “Multi-channel music separation with deep neural networks,” in *Proc. of 24th European Signal Processing Conference (EUSIPCO)*, 2016, pp. 1748–1752.
- [26] N. Takahashi and Y. Mitsufuji, “Densely connected multidilated convolutional networks for dense prediction tasks,” in *Proc. of IEEE/CVF Conference on Computer Vision and Pattern Recognition (CVPR)*, 2021, pp. 993–1002.
- [27] N. Takahashi and Y. Mitsufuji, “D3Net: Densely connected multidilated DenseNet for music source separation,” *arXiv*, vol. abs/2010.01733, 2020.
- [28] F.-R. Stöter, A. Liutkus, and N. Ito, “The 2018 signal separation evaluation campaign,” in *International Conference on Latent Variable Analysis and Signal Separation*. Springer, 2018, pp. 293–305.
- [29] F. Lluís, J. Pons, and X. Serra, “End-to-End Music Source Separation: Is it Possible in the Waveform Domain?,” in *Proc. of Interspeech*, 2019, pp. 4619–4623.
- [30] D. Stoller, S. Ewert, and S. Dixon, “Wave-U-Net: A Multi-Scale Neural Network for End-to-End Audio Source Separation,” in *Proc. of the 19th International Society for Music Information Retrieval (ISMIR) Conference*, 2018, pp. 334–340.
- [31] A. Défossez, N. Usunier, L. Bottou, and F. Bach, “Demucs: Deep extractor for music sources with extra unlabeled data remixed,” *arXiv*, 2019.
- [32] Y. N. Dauphin, A. Fan, M. Auli, and D. Grangier, “Language modeling with gated convolutional networks,” in *Proc. of the 34th International Conference on Machine Learning (ICML)*, 2017, vol. 70, pp. 933–941.
- [33] M. Kim, W. Choi, J. Chung, D. Lee, and S. Jung, “KUIELab-MDX-Net: A Two-Stream Neural Network for Music Demixing,” in *Proc. of the International Society for Music Information Retrieval (ISMIR) Conference Workshop on Music Source Separation*, 2021.
- [34] C.-Y. Yu and K.-W. Cheuk, “Danna-Sep: Unite to separate them all,” in *Proc. of the International Society for Music Information Retrieval (ISMIR) Conference Workshop on Music Source Separation*, 2021.
- [35] S. Uhlich, M. Porcu, F. Giron, M. Enenkl, T. Kemp, N. Takahashi, and Y. Mitsufuji, “Improving music source separation based on deep neural networks through data augmentation and network blending,” in *Proc. of IEEE International Conference on Acoustics, Speech and Signal Processing (ICASSP)*, 2017, pp. 261–265.
- [36] W. Choi, M. Kim, J. Chung, and S. Jung, “LaSAFT: Latent Source Attentive Frequency Transformation For Conditioned Source Separation,” in *Proc. of IEEE International Conference on Acoustics, Speech and Signal Processing (ICASSP)*, 2021, pp. 171–175.
- [37] Y.-S. Jeong, J. Kim, W. Choi, J. Chung, and S. Jung, “LightSAFT: Lightweight Latent Source Aware Frequency Transform for Source Separation,” in *Proc. of the International Society for Music Information Retrieval (ISMIR) Conference Workshop on Music Source Separation*, 2021.
- [38] H. Liu, Q. Kong, and J. Liu, “CWS-PResUNet: Music Source Separation with Channel-wise Subband Phase-aware ResUNet,” in *Proc. of the International Society for Music Information Retrieval (ISMIR) Conference Workshop on Music Source Separation*, 2021.
- [39] W. Choi, M. Kim, J. Chung, D. Lee, and S. Jung, “Investigating U-Nets with various intermediate blocks for spectrogram-based singing voice separation,” in *Proc. of the 21st International Society for Music Information Retrieval (ISMIR) Conference*, 2020, pp. 192–198.
- [40] O. Ronneberger, P. Fischer, and T. Brox, “U-Net: Convolutional Networks for Biomedical Image Segmentation,” in *Proc. of Medical Image Computing and Computer-*

Assisted Intervention (MICCAI), 2015, pp. 234–241.

- [41] A. Défossez, “Hybrid spectrogram and waveform source separation,” in *Proc. of the International Society for Music Information Retrieval (ISMIR) Conference Workshop on Music Source Separation*, 2021.
- [42] Q. Kong, Y. Cao, H. Liu, K. Choi, and Y. Wang, “Decoupling Magnitude and Phase Estimation with Deep ResUNet for Music Source Separation,” in *Proc. of the 22nd International Society for Music Information Retrieval (ISMIR) Conference*, 2021, pp. 342–349.
- [43] N. Takahashi, P. Agrawal, N. Goswami, and Y. Mitsufuji, “PhaseNet: Discretized Phase Modeling with Deep Neural Networks for Audio Source Separation,” in *Proc. Interspeech*, 2018, pp. 2713–2717.
- [44] D. Yin, C. Luo, Z. Xiong, and W. Zeng, “Phasen: A phase-and-harmonics-aware speech enhancement network,” in *Proc. AAAI*, 2020, p. 9458–9465.
- [45] T. Peer, S. Welker, and T. Gerkmann, “DiffPhase: Generative Diffusion-based STFT Phase Retrieval,” *arXiv*, vol. abs/2211.04332, 2022.
- [46] H.-S. Choi, J.-H. Kim, J. Huh, A. Kim, J.-W. Ha, and K. Lee, “Phase-aware speech enhancement with deep complex U-net,” *arXiv*, 2019.
- [47] R. Caruana, “Multitask learning,” *Mach. Learn.*, vol. 28, no. 1, pp. 41–75, jul 1997.
- [48] Z. Rafii, A. Liutkus, F.-R. Stöter, S. I. Mimilakis, and R. Bittner, “The MUSDB18 corpus for music separation,” Dec. 2017.
- [49] D. P. Kingma and J. Ba, “Adam: A method for stochastic optimization,” in *Proc. of 3rd International Conference on Learning Representations (ICLR)*, Y. Bengio and Y. LeCun, Eds., 2015.



Ryosuke Sawata (S’15–M’16) received his B.S. and M.S. degrees in Electronics and Information Engineering from Hokkaido University, Japan in 2014 and 2016, respectively. He is currently a researcher at Sony Group Corporation and Ph.D. candidate at Graduate School of Information Science and Technology, Hokkaido University. His research interests include biosignal processing, music information retrieval and acoustic signal processing. He is a member of IEEE.



Naoya Takahashi received Ph.D. from University of Tsukuba, Japan, in 2020. Formerly, he had worked at the Computer Vision Lab at ETH Zurich, Switzerland. Since he joined Sony in 2008, he has performed research in the field of audio, computer vision, and machine learning. In 2018, he won the Sony Outstanding Engineer Award, which is the highest form of individual recognition for Sony Group engineers. He achieved the best scores in several challenges including Signal Separation Evaluation Campaign (SiSEC) 2018, and Detection and

Classification of Acoustic Scenes and Events (DCASE) 2021. He has authored several papers and served as a reviewer at CVPR, ICASSP, Interspeech, ICCV, Trans. ASLP, Trans. MM, and more. He co-organized the DCASE 2022 task3.



network compactization.

Stefan Uhlich received the Dipl.-Ing. and PhD degree in electrical engineering from the University of Stuttgart, Germany, in 2006 and 2012, respectively. From 2007 to 2011 he was a research assistant at the Chair of System Theory and Signal Processing, University of Stuttgart. In this time he worked in the area of statistical signal processing, focusing especially on parameter estimation theory and methods. Since 2011, he is with the Sony Stuttgart Technology Center where he works as a Principal Engineer on problems in music source separation and deep neural



from movies by Sony Pictures Entertainment were used for the evaluation.

Shusuke Takahashi received his B.E. degree in communications engineering and M.S. degree in information science from Tohoku University, Japan, in 2000 and 2002, respectively. He is currently a researcher and a senior manager at Sony Group Corporation, Japan. His research interests include speech and audio signal processing and machine learning. His team achieved the first place in DCASE 2021 Challenge in Task3, and co-organized DCASE Challenge in 2022 and 2023. He also co-organized Sound Demixing Challenge 2023, where real audio



audio solution called “Sonic Surf VR”. He also won several awards such as TIGA award for best audio design for Gran Turismo Sports, and a jury selection at Japan Media Arts Festival for their 576-channel sound field synthesis called “Acoustic Vessel Odyssey”. From 2011 to 2012, he was a visiting researcher at Analysis/Synthesis Team, Institut de Recherche et Coordination Acoustique/Musique (IRCAM), Paris, France. He was involved in the 3DTV content search project sponsored by European Project FP7, in research collaboration with IRCAM. In 2021, his team organized Music Demixing (MDX) Challenge where Sony Music provided a professionally-produced music dataset for the evaluation of submitted systems to an online platform on AICrowd. His team also participated in DCASE2021 Challenge and achieved the first place in Task3.

Yuki Mitsufuji received the BS and MS degrees in information science from Keio University in 2002 and 2004, respectively. He obtained the PhD degree in information science and technology from the University of Tokyo in 2020. Currently, he is leading Creative AI Lab at Sony Group Corporation while serving as Specially Appointed Associate Professor at Tokyo Institute of Technology. He joined Sony Corporation in 2004 and has been leading teams that developed the sound design for the PlayStation game title called “Gran Turismo Sport”, and spatial